REPORT DOCUMENTATION PAGE		READ INSTRUCTIONS BEFORE COMPLETING FORM
1. REPORT NUMBER NRL Memorandum Report 4892	2. GOVT ACCESSION NO. AD-A118163	3. RECIPIENT'S CATALOG NUMBER
4. TITLE (and Subtitle) PSEUDOSPECTRAL SOLUTION OF ONE DIMENSIONAL AND TWO DIMENSIONAL INVISCID FLOWS WITH SHOCK WAVES		5. TYPE OF REPORT & PERIOD COVERED Interim report on a continuing NRL problem.
		6. PERFORMING ORG. REPORT NUMBER
7. AUTHOR(s) L. Sakell		8. CONTRACT OR GRANT NUMBER(s)
9. PERFORMING ORGANIZATION NAME AND ADDRESS Naval Research Laboratory Washington, DC 20375		10. PROGRAM ELEMENT, PROJECT, TASK AREA & WORK UNIT NUMBERS 61153N-13; RR013-02-42; 58-1374-0-0
11. CONTROLLING OFFICE NAME AND ADDRESS Office of Naval Research Arlington, VA 22217		12. REPORT DATE August 6, 1982
		13. NUMBER OF PAGES 33
14. MONITORING AGENCY NAME & ADDRESS(if different from Controlling Office)		15. SECURITY CLASS. (of this report) UNCLASSIFIED
		15a. DECLASSIFICATION/DOWNGRADING SCHEDULE

16. DISTRIBUTION STATEMENT (of this Report)

Approved for public release; distribution unlimited.

17. DISTRIBUTION STATEMENT (of the abstract entered in Block 20, if different from Report)

18. SUPPLEMENTARY NOTES

19. KEY WORDS (Continue on reverse side if necessary and identify by block number)

Pseudospectral	Shock waves
Euler equations	Chebyshev
Inviscid flow	Artificial viscosity

20. ABSTRACT (Continue on reverse side if necessary and identify by block number)

A new approach is presented for the utilization of pseudospectral techniques for the solution of inviscid flows with shock waves using the full Euler equations of motion. Artificial viscosity is applied together with low pass spectral filtering to damp out pre and post cursor numerical oscillations. Solutions are presented for the one dimensional propagating shock wave problem and for two dimensional supersonic wedge flows.

DD FORM 1473 EDITION OF 1 NOV 65 IS OBSOLETE
1 JAN 73
S/N 0102-014-6601

CONTENTS

Accession For

NTIS GRA&I	X
DTIC TAB	☐
Unannounced	☐
Justification_____	

By_____
Distribution/

Availability Codes

| Dist | Avail and/or Special |
| A | |

DTIC
COPY
INSPECTED
2

PSEUDOSPECTRAL SOLUTION OF ONE DIMENSIONAL AND TWO DIMENSIONAL INVISCID FLOWS WITH SHOCK WAVES

I. INTRODUCTION

Pseudospectral techniques have been used to solve the one dimensional propagating shock wave problem. Taylor et al (Reference 1) and Gottlieb et al (Reference 2) have done so using the Euler equations of motion. Taylor utilized the FCT (Flux Corrected Transport) algorithm of Boris and Book (Reference 3) to damp out unwanted numerical oscillations. This procedure yielded broadening of the shock wave. They treated a Mach 1.4 shock wave propagating into a free stream at rest. The flow behind the shock wave was subsonic. Gottlieb et al treated the shock tube problem for shock wave Mach numbers of 2.1 and 29.3. The free stream was subsonic with the flow behind the shock wave being supersonic for both mach number cases. They performed a detailed analysis of the effects of different filtering techniques on reducing unwanted numerical oscillations. They considered the Shuman filter given by:

$$\overline{U}_j^n = U_j^n + \theta_{j+1/2}\,[U_{j+1}^n - U_j^n] + \theta_{j-1/2}\,[U_j^n - U_{j-1}^n] \qquad (1)$$

$\overline{U}_j^n$ is the filtered conservative variable at the jth spatial location and the nth time step. For a two dimensional problem one would need to filter in each direction separately. The $\theta_{j+1/2}$ coefficients are given by

$$\theta_{j+\frac{1}{2}} = \beta \frac{\left| \rho_{j+2} - \rho_{j+1} - 2(\rho_{j+1} - \rho_j) + (\rho_j - \rho_{j-1}) \right|}{\left| \rho_{j+2} - \rho_{j+1} \right| + 2\left| \rho_{j+1} - \rho_j \right| + \left| \rho_j - \rho_{j-1} \right|} \qquad (2)$$

and β is a constant greater than zero and less than one. Beta was chosen to be 0.01. The above was used in one of two versions, constant $\theta_{j\pm\frac{1}{2}}$ coefficients and variable $\theta_{j\pm\frac{1}{2}}$ coefficients. The former is qualitatively equivalent to a first order artificial viscosity scheme. Both were applied to the physical variables directly. They also utilized a low pass spectral filter, which they developed, to damp out the oscillations which arose from the highest frequency spectral components. The form of their spectral filter is:

$$e^{-\alpha \left[\frac{k-k_o}{k_{max}-k_o} \right]} \qquad (3)$$

where k is the spectral wavenumber, k_{max} is the maximum wavenumber corresponding to the total number of collocation points and $k_o = \frac{5}{6} N$ where N is the total number of collocation points used to represent the flow. The spectral filter was applied first, followed by the Shuman filter. They determined rules for applying the low pass spectral filter. They found that applying it over the highest sixth of the frequency values gave good results. The Shuman filtering employed was one sided. That is, the shock position was determined first and then the filter was applied over the region behind the shock wave and separately to the region in front of the shock wave. Using this approach they were able to obtain a sharp shock with the correct propagation velocity. Both approaches, however, have some drawbacks. The former did not yield a sharp discontinuity while the latter

required an examination of the spectral coefficients at each time step to determine the shock wave location in order to avoid applying the physical space filter across the shock front. When more general classes of inviscid flows are treated (ones with complex, multiple shock geometries) the smearing in the first approach may prove unacceptable. The one-sided smoothing of the latter will become cumbersome to employ.

A brief outline of pseudospectral techniques will be given in Section 2. The third section of this report will present results for the one dimensional propagating shock wave problem using a different physical space smoothing function than either of the above while retaining the lowpass spectral filtering technique of Reference 2. An artificial viscosity scheme is used uniformly throughout the entire flow field, including across the shock front, to resolve the shock wave as a sharp discontinuity and at the same time maintain the correct shock propagation velocity.

To further demonstrate the utility of this approach to the solution of flows by pseudospectral methods, solutions to two-dimensional inviscid supersonic wedge flows will also be presented in Section 4 of this report. To the present author's knowledge, this is the first time pseudospectral solution techniques have been used to successfully treat two-dimensional inviscid flows.

2. PSEUDOSPECTRAL METHODS

A brief description of pseudospectral techniques will be presented here for completeness. For those readers interested in a detailed exposition on pseudospectral techniques, Reference 4 is strongly recommended.

Pseudospectral techniques involve the use of series of functions to solve differential equations. For all work reported herein, Chebyshev polynomials are used. Chebyshev polynomials are represented by $T_n(x)$ and are given by:

$$T_n(x) = \cos [n \cos^{-1}(x)]$$
$$= \cos [n \; \theta] \qquad \text{(4a)}$$

where
$$\theta = \cos^{-1}(x)$$

The Chebyshev polynomials have the following property:

$$2 \, T_n(x) = \frac{T'_{n+1}(x)}{n+1} - \frac{T'_{n-1}(x)}{n-1} \qquad \text{(4b)}$$

Chebyshev polynomials may be used to represent a function $F(x)$ in the following manner

$$F(x) = \sum_{n=0}^{N} A_n T_n(x) \qquad \text{(5)}$$

A function $F(x,t)$ may be represented as:

$$F(x,t) = \sum_{n=0}^{N} A_n(t) \, T_n(x) \qquad \text{(6)}$$

where the time dependence is totally contained in the series coefficients $A_n(t)$, and the x dependence in the Chebyshev functions $T_n(x)$.

Let us now consider the application of such techniques for the solution of the one-dimensional unsteady Euler equation in conservation law form:

$$\frac{\partial \vec{U}}{\partial t} + \frac{\partial \vec{E}}{\partial x} = 0 \tag{7a}$$

where

$$\vec{U} = \begin{bmatrix} \rho \\ \rho u \\ e \end{bmatrix} \qquad \vec{E} = \begin{bmatrix} \rho u \\ p + \rho u^2 \\ (e+p)u \end{bmatrix} \tag{7b}$$

and

$$e = \frac{p}{(\gamma - 1)} + \frac{\rho}{2} u^2 \tag{7c}$$

The pseudospectral solution, using Chebyshev collocation, of this equation involves using Chebyshev series to obtain the spatial derivative and finite difference algorithms to obtain the time derivative. (A flowchart of the solution procedure is shown in Figure 1). Collocation involves the specification of the initial flow variables and the computation of the time dependent solution for the flow variables at distinct pre-determined spatial positions or points. These positions are the collocation points. The spatial derivative is obtained as follows. At t_o the values of $\vec{E}(x)$ at the collocation points x_j are specified.

The collocation points are given by

$$x_j = \cos\left(\frac{\pi j}{N}\right) \qquad 0 < j < N \tag{8}$$

where N is the total number of Chebyshev polynomials one chooses to use to represent the function $\vec{E}(x)$. As can easily be seen, the x_j points are not evenly spaced, but are clustered about $x = \pm 1$.

We represent $\vec{E}(x)$ by

$$\vec{E}(t,x) = \sum_{n=o}^{N} A_n(t) T_n(x) \tag{9}$$

5

The left hand side of this equation is known while the A_n's are at this point unknown. The first step is therefore to solve for the A_n's for each $\vec{E}(x)$ vector element. This could be done by a simple matrix inversion. However, it is much faster to use FFT's (fast Fourier transforms). We therefore use the FFT's to invert (9) to obtain the values of the A_n's. We may then represent the spatial derivative $\partial E/\partial X$ as a Chebyshev series given by:

$$\frac{\partial E}{\partial X} = \sum_{n=0}^{N} A_n^{(1)} T_n(x) \qquad (10)$$

Because of properties of Chebyshev polynomials (equation 4b) we may relate the spectral coefficients of the spatial derivative, $A_n^{(1)}$, to the known spectral coefficients of $\vec{E}$, namely A_n, by the following recurrence relation.

$$A_n^{(1)} = \frac{2}{C_n} \sum_{\substack{p=n+1 \\ p+n=odd}}^{N} p A_p \qquad (11)$$

Since the A_n's are known at the current time step t_o (not necessarily zero) from Equation 9, the $A_n^{(1)}$'s are obtained from the recurrence relation, Equation 11. The summation in Equation 10 is performed using the FFT. Therefore it remains only to calculate the temporal derivative $\frac{\partial \vec{U}}{\partial t}$ in (7). For the results presented herein the Adams-Bashforth algorithm was used to advance the solution to $t_o + \Delta t$. (The modified Euler predictor corrector scheme was also investigated. However, it did not yield better results and took more computer time to implement.) This process is then cyclically repeated to march the solution in time (physical or computational). The

Adams-Bashforth algorithm is given by:

$$\vec{U}^{t+\Delta t} = \vec{U}^t + \frac{3}{2} \Delta t \left(\frac{\partial \vec{E}}{\partial x}\right)^t - \frac{1}{2} \Delta t \left(\frac{\partial \vec{E}}{\partial x}\right)^{t-\Delta t} \tag{12}$$

where superscripts denote the value of time at which each term is evaluated.

3. ONE DIMENSIONAL PROPAGATING SHOCK WAVE RESULTS

Two types of artificial viscosity schemes were tried; a second order scheme given by

$$D_{n,i} = -\mu \left(U_{n,i+1} - 2U_{n,i} + U_{n,i-1}\right) \tag{13}$$

and a fourth order scheme given by

$$D_{n,i} = -\mu \left\{U_{n,i+2} + U_{n,i-2} - 4 \left[U_{n,i+1} + U_{n,i-1}\right] + 6 U_{n,i}\right\} \tag{14}$$

where $D_{n,i}$ is the magnitude of the dissipation for the nth conservative flow variable at the ith spatial point. In both cases, μ is the magnitude of the artificial viscosity.

Three types of shock tube flows were considered: (a) supersonic inflow/outflow, (b) subsonic inflow/outflow and (c) supersonic inflow/subsonic outflow. They represent the entire range of shock tube problems and will be discussed below. The time step size used throughout was one half the maximum based on stability considerations (effectively a Courant number of 0.5). The resulting time step size values are (a) $.502 \times 10^{-4}$, (b) $.998 \times 10^{-4}$ and (c) $.574 \times 10^{-4}$.

7

The conditions for the supersonic inflow/outflow case were a free
stream Mach number of 1.5 and a shock Mach number of 3.5 (with respect to
ground fixed coordinates). One hundred twenty eight Chebyshev polynomial
terms were used to represent the flow. All results utilized the low pass
spectral filter. In all cases the initial shock position ($t = t_o = 0$)
was at $x = -1.0$ (i.e. at the left hand side computational boundary).

The second order artificial viscosity scheme was used first for the
above problem. Typical results are shown in Figure 2 where the static
pressure distribution (non-dimensionalized by the free stream va $> p_1$) is
shown. P_2 represents the post shock static pressure. The anal $\cdot$ shock
wave position at $t = .1505$ is shown for comparison. Clearly the ε wave is
unacceptably smeared. For this reason the second order smoothi $\cdot$ eme was
abandoned.

Results for this case with the fourth order smoothing are shown in
Figures 3 and 4. The figures show the calculated shock solution at times of
0.05 and 0.15 respectively. The analytic shock position at the respective
times is shown for comparison. As can be seen, the computed shock position
is in excellent agreement with the analytic solution. Further, the correct
pre and post shock pressures are maintained. One can see the effect of grid
resolution by comparing Figures 3 and 4. As previously mentioned in Section
2 points are clustered about $x = \pm 1$ with the coarsest grid spacing
occurring at $x = 0$. The shock wave is in a region of high point resolution in
Figure 3 and nearly at the most coarse grid resolution in Figure 4. The
apparent skewness of the calculated shock front in Figure 4 is not due to
overly large dissipation. It is instead due to the coarse grid spacing.

8

The shock cannot of course be resolved to within a single grid spacing. All flow properties were held fixed at both the supersonic inflow and outflow boundaries. At the supersonic outflow boundary it was necessary to apply the second order artificial viscosity locally in order to remove oscillations emanating from this boundary. Without this localized second order smoothing, the solution went catastrophically unstable at the outflow boundary.

The second shock tube problem considered involved supersonic inflow and subsonic outflow (see Figures 5 and 6). The free stream Mach number was 0.845 with the shock Mach number 2.949 with respect to the ground. Again the shock is maintained as a sharp discontinuity propagating at the correct velocity. As before, the supersonic inflow boundary conditions are all flow variables held fixed. However, at the subsonic outflow boundary one physical flow variable was specified with the remaining ones computed from the characteristic values of the flow (as in Reference 2).

The last shock tube problem considered had both subsonic inflow and subsonic outflow. The free stream mach number was 0.5 while the shock wave Mach number was 1.8 with respect to the ground. Results for the pressure distribution at two different times are shown in Figures 7 and 8. As in previous cases, the shock position and shape are in excellent agreement with the analytical values. The boundary conditions used were to hold all flow variables fixed at the subsonic inflow boundary and (as in the previous case) to hold one flow variable fixed at the subsonic outflow boundary while computing the remaining ones from the characteristics.

4. TWO DIMENSIONAL SUPERSONIC WEDGE FLOW RESULTS

Two cases were considered, a ten degree half angle wedge at free stream Mach numbers of 1.5 and 3.0. The computational grid was dimensioned 33 x 33. The resulting grid lines are plotted in Figure 9. Figure 10 shows the allignment of the computational boundary in physical space. Now, since

$$x_1 \leqslant x \leqslant x_2$$

$$o \leqslant y \leqslant y_{max}$$

(15)

we must transform to (ξ, η) space to obtain $|\xi| < 1$, $|\eta| < 1$, which is required of the collocation points. This transformation is given by:

$$\xi = \frac{2x-(x_1+x_2)}{(x_2-x_1)}$$

$$\eta = \frac{2y-y_{max}}{y_{max}}$$

(16)

No attempt was made to use the optimum time step size, given by Reference 5.

$$(\Delta t)_{max} \leqslant \frac{8.0}{N^2 |u+c|_{max}}$$

(17)

In fact, for all calculations presented herein, an effective Courant number of 0.5 was used. (That is, the numerator of (17) was replaced by 4.0.) For purposes of comparison, the wedge surface pressure and density distributions as well as computer generated contour plots of the shock wave position and

10

shape are used. Fourth order dissipation was used throughout in both the x and y directions. Second order dissipation was used in the neighborhood of $x = x_2$ (in the x-direction only) to eliminate oscillations emanating from the supersonic outflow boundary. The flow internal to the computational boundaries was initialized to free stream values. Along region BCDE of the computational boundary the flow was held fixed at free stream values. Along region AB and FE it was held fixed at wedge flow properties. Finally at the wedge surface, region AF, surface tangency was imposed after each time step.

Results for the Mach 1.5 case are shown in Figures 11 through 14. The time step size was $.125 \times 10^{-2}$. Figures 11 and 12 show contour plots of the pressure and density fields respectively. The analytic shock position is also shown as a solid line for comparison. The shock position and orientation are predicted exactly by the pseudospectral solution. The wide band or thickness of the computed shock is due to the very coarse grid resolution used in the 2D runs, namely 33x33. In terms of grid intervals the shock shown in Figures 11 and 12 lies over only two to three grid intervals. Increasing the grid resolution will reduce the thickness of the contoured shock wave.

The increase in shock thickness which appears in Figures 11 and 12 in the neighborhood of the right hand side computational boundary is due to the localized second order artificial viscosity scheme used in that region (supersonic outflow). With a 33 point resolution along the x-axis only several points are needed to physically extend well into the interior of the computational area. With a more realistic grid resolution, say 128 points, the maximum extent would be reduced to only $x = 0.99$ and no effect would be

11

present in the shock plots. Surface pressure and density distributions are shown in Figures 13 and 14. In both cases, agreement between the computed result and the analytic result (represented by the dotted line) is excellent. The minor overshoots and undershoots that appear in both plots represent differences of less that 1.5% from the analytic values.

Similar plots are shown in Figures 15 through 18 for the Mach 3.0 case. The time step size is $.785 \times 10^{-3}$. Agreement is excellent both in the shock shape and location and in the surface pressure and density distributions.

5. CONCLUSIONS

(1) Pseudospectral solution techniques can treat inviscid 1-D and 2-D flows with shock waves quite accurately when a low pass spectral filter is used in conjunction with a fourth order artificial viscosity scheme (applied to the physical variables). All shocks are maintained as discontinuities with only minor pre and post cursor oscillations.

(2) For the 2D flow problem considered here (as well as the 1D supersonic outflow problem), a localized second order artificial viscosity scheme must be applied in the neighborhood of the supersonic outflow boundary to damp out oscillations that arise at the boundary and keep the solution stable. Without it, the solution always goes catastrophically unstable at this boundary.
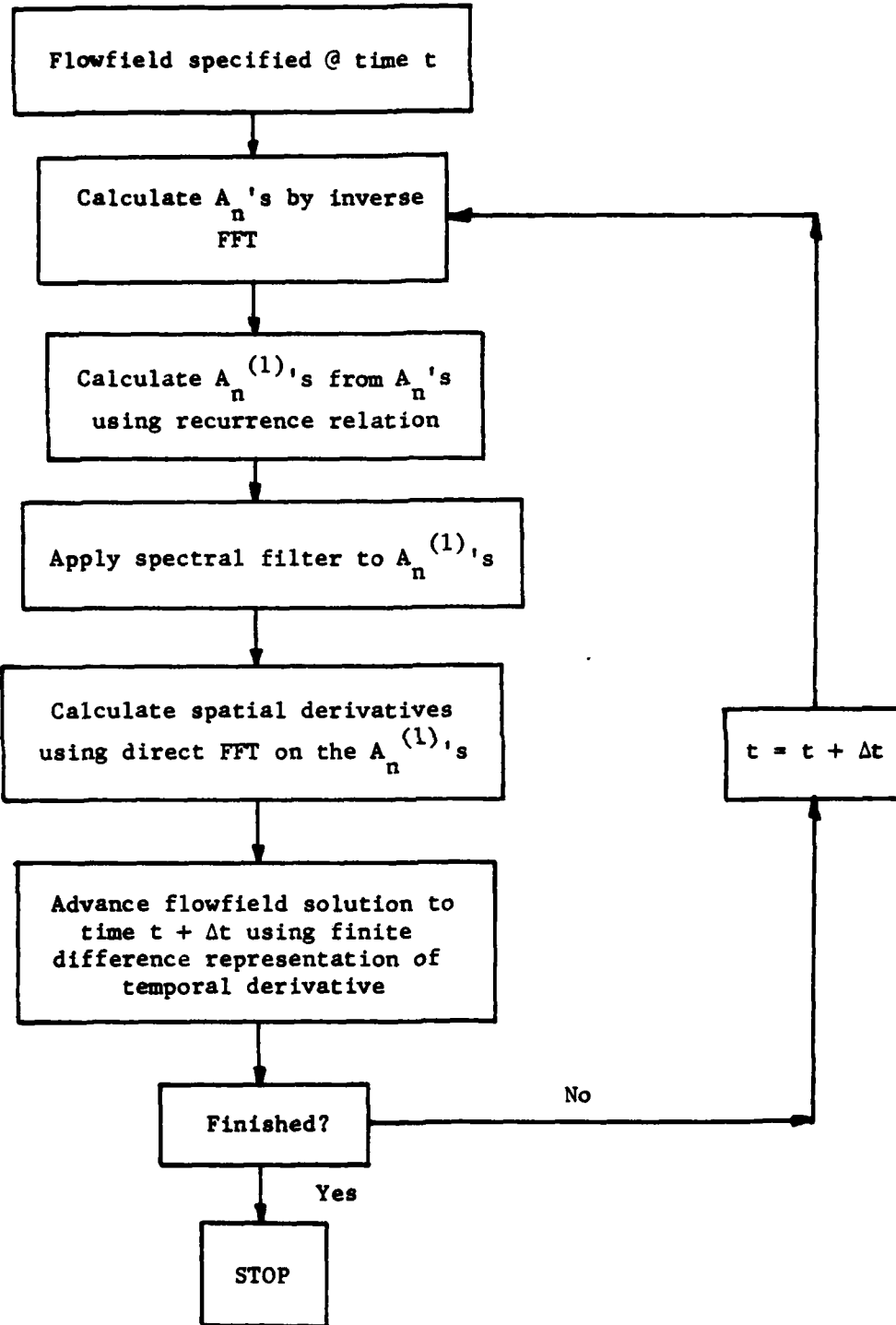
```
┌─────────────────────────────┐
│  Flowfield specified @ time t │
└─────────────────────────────┘
              │
              ▼
┌─────────────────────────────┐
│  Calculate Aₙ's by inverse   │◄───────┐
│  FFT                         │        │
└─────────────────────────────┘        │
              │                         │
              ▼                         │
┌─────────────────────────────┐        │
│  Calculate Aₙ⁽¹⁾'s from Aₙ's │        │
│  using recurrence relation   │        │
└─────────────────────────────┘        │
              │                         │
              ▼                         │
┌─────────────────────────────┐        │
│  Apply spectral filter to    │        │
│  Aₙ⁽¹⁾'s                     │        │
└─────────────────────────────┘        │
              │                         │
              ▼                   ┌──────────┐
┌─────────────────────────────┐  │ t = t + Δt│
│  Calculate spatial derivatives│ └──────────┘
│  using direct FFT on the     │        ▲
│  Aₙ⁽¹⁾'s                     │        │
└─────────────────────────────┘        │
              │                         │
              ▼                         │
┌─────────────────────────────┐        │
│  Advance flowfield solution to│       │
│  time t + Δt using finite     │       │
│  difference representation of │       │
│  temporal derivative          │       │
└─────────────────────────────┘        │
              │                         │
              ▼              No         │
       ┌──────────┐─────────────────────┘
       │ Finished?│
       └──────────┘
              │ Yes
              ▼
        ┌────────┐
        │  STOP  │
        └────────┘
```

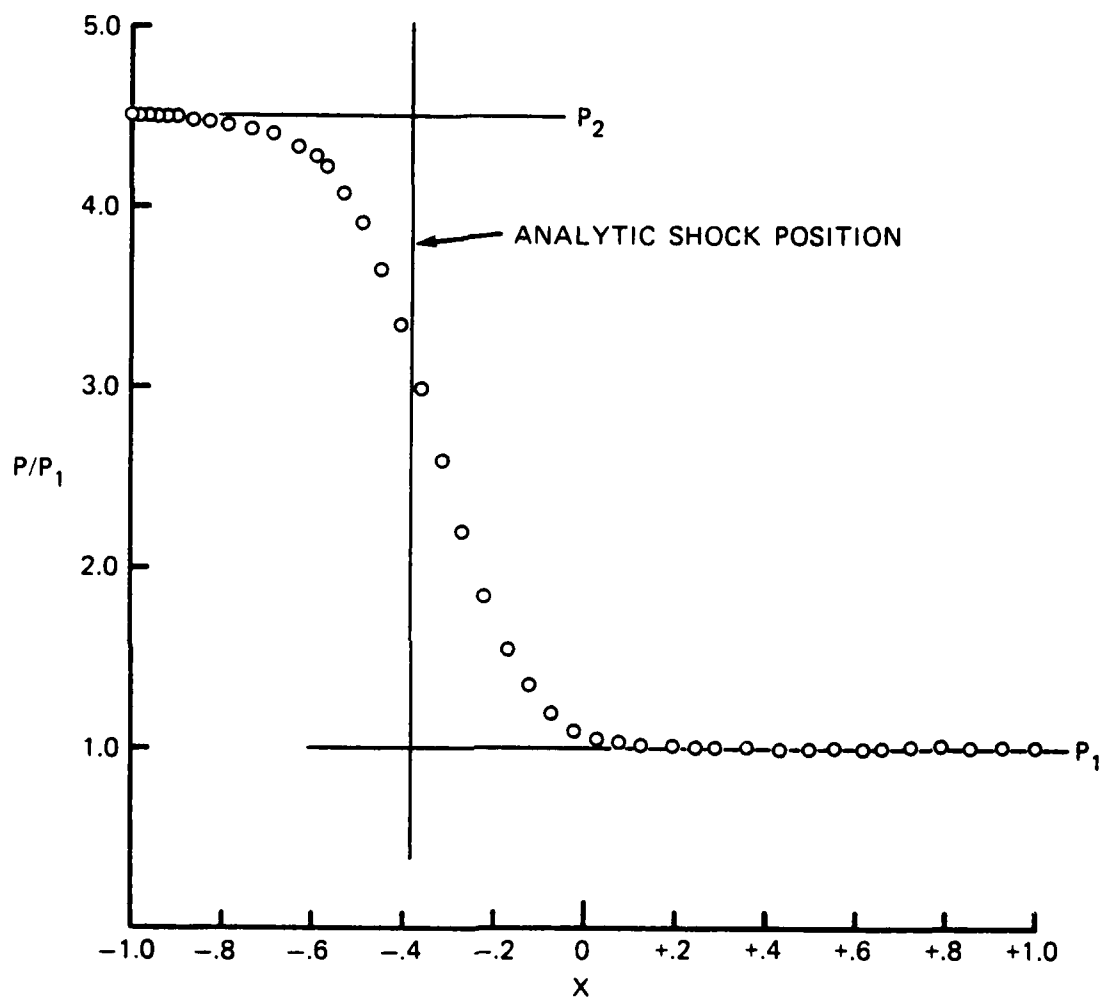Fig. 1 — Pseudospectral calculation flowchart

Fig. 2 — P/P_1 vs x at ITER = 3000, t = 0.1505 for supersonic inflow and outflow.
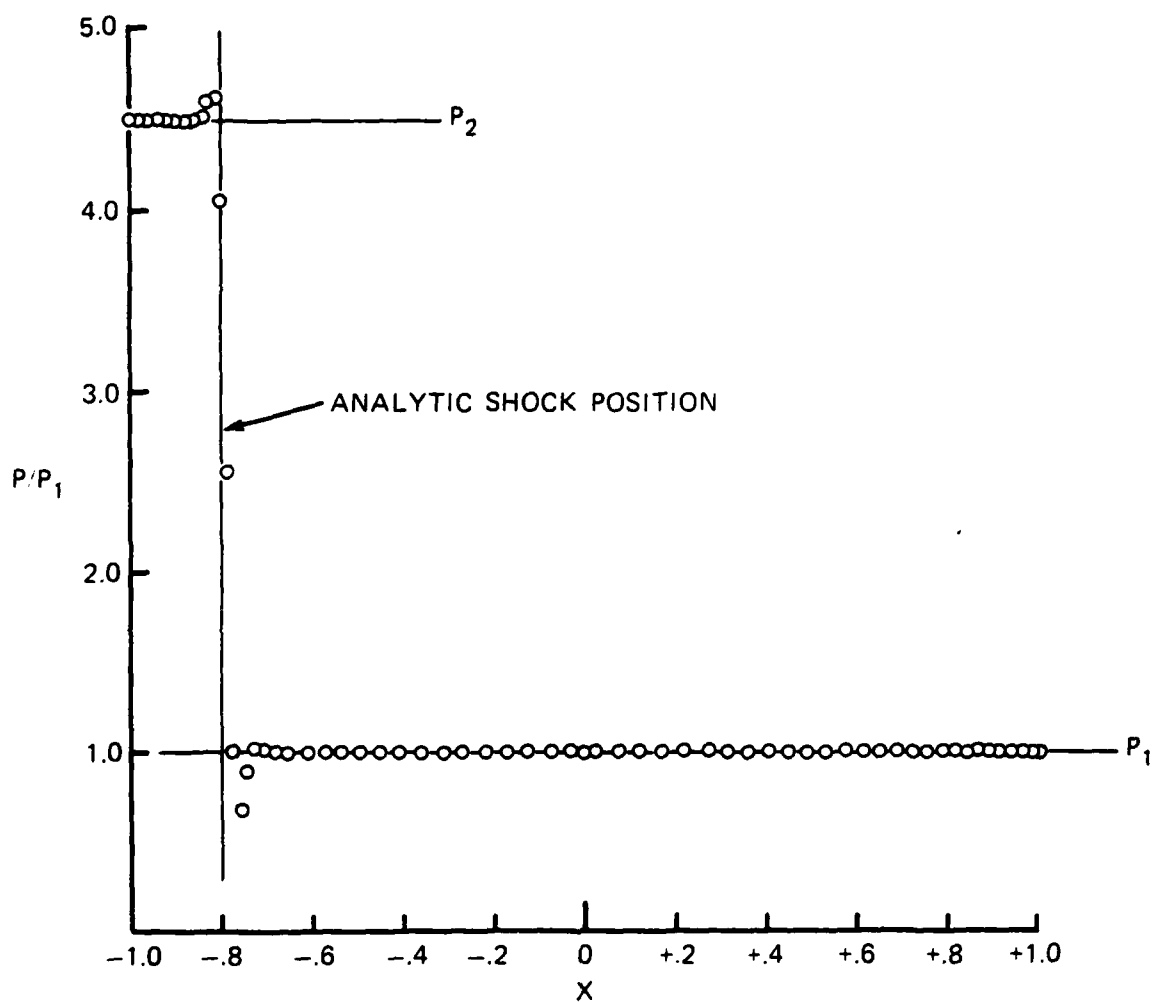MSHOCK = 3.5, M1 = 1.5, 2nd order dissipation scheme.

14

Fig. 3 — P/P_1 vs x at ITER = 1000, t = 0.0501 for supersonic inflow and outflow. MSHOCK = 3.5, M1 = 1.5, 4th order dissipation scheme.
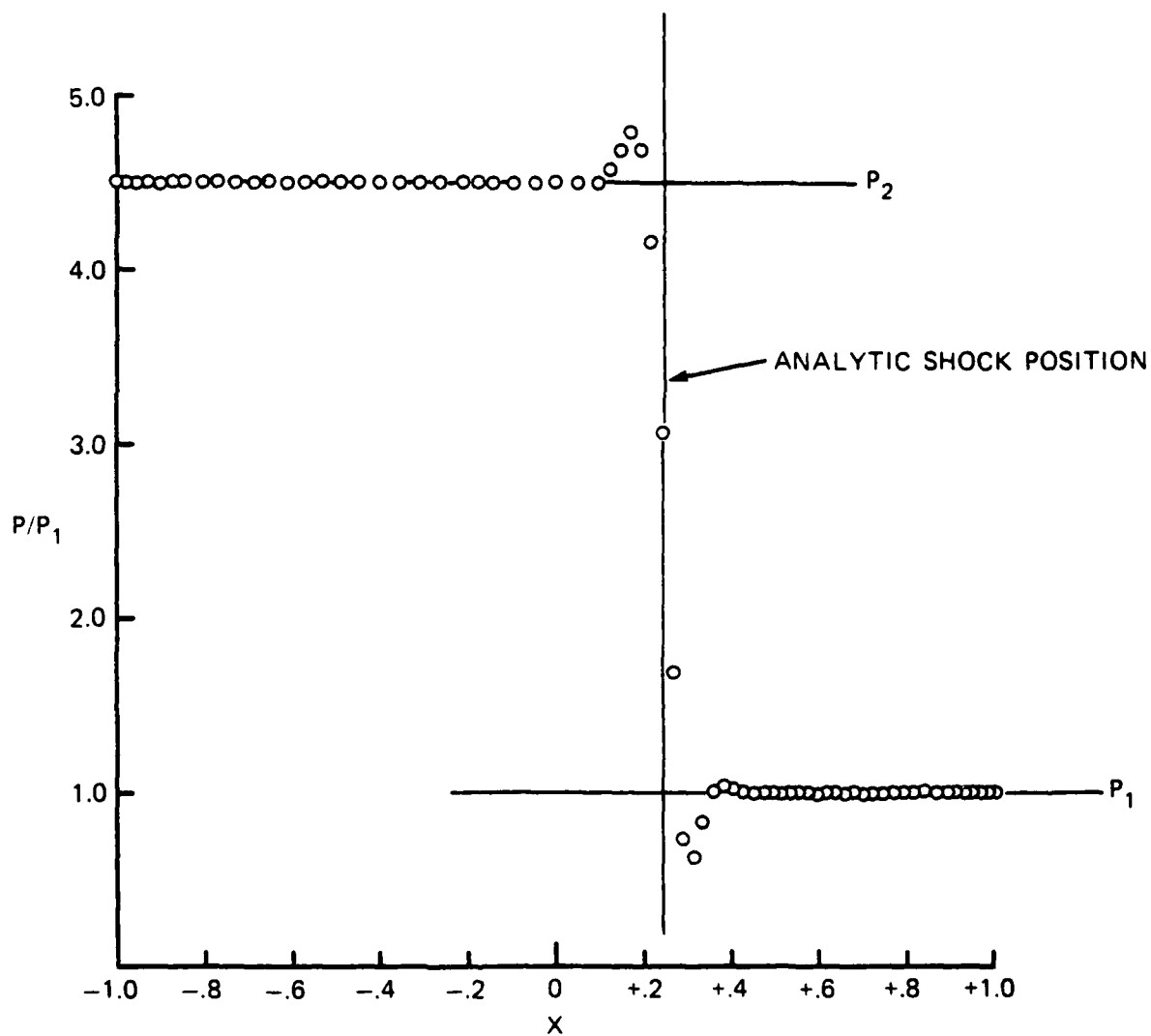
Fig. 4 — P/P_1 vs x at ITER = 6000, t = 0.3010 for supersonic inflow and outflow. MSHOCK = 3.5, M1 = 1.5, 4th order dissipation scheme.
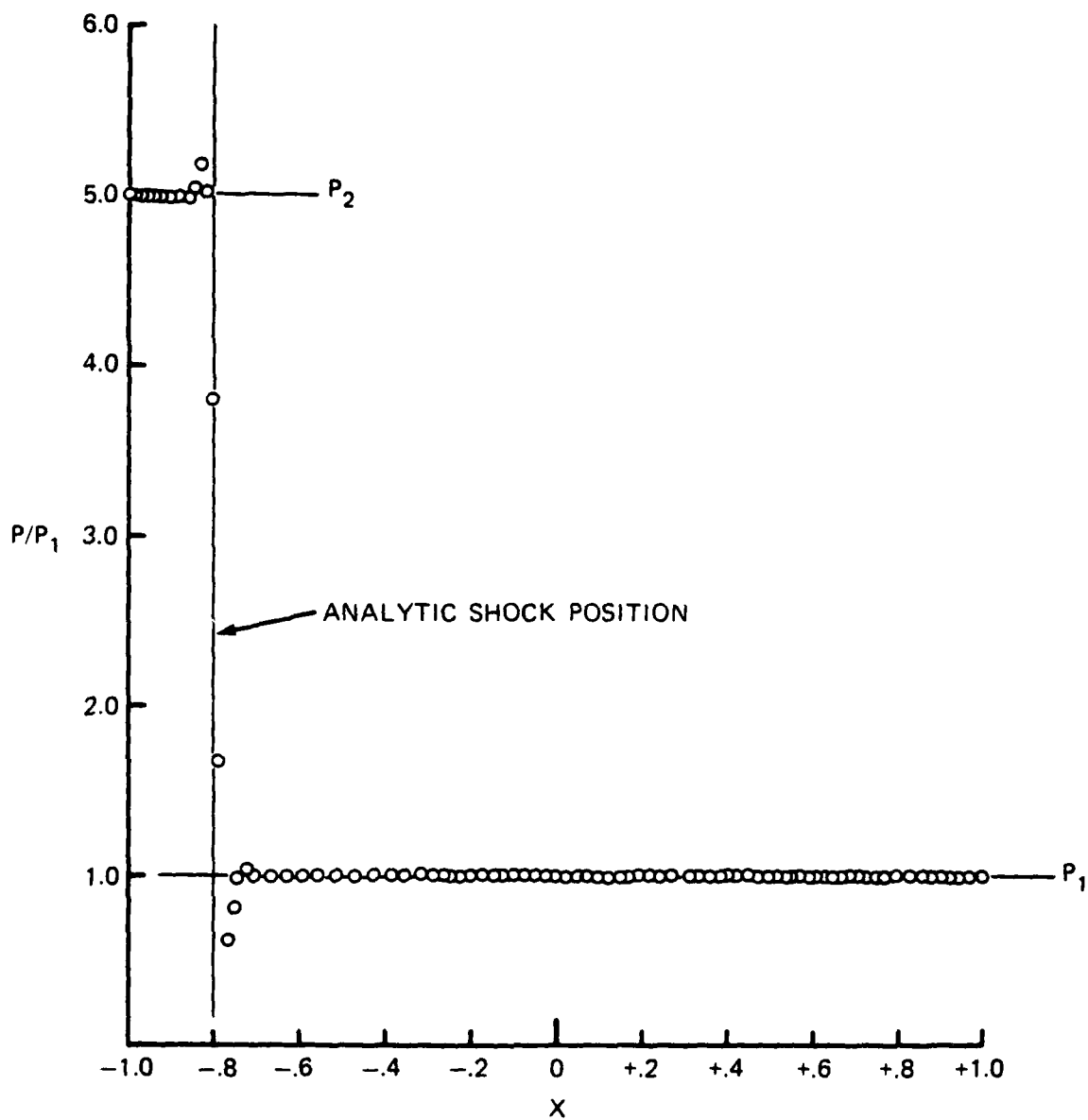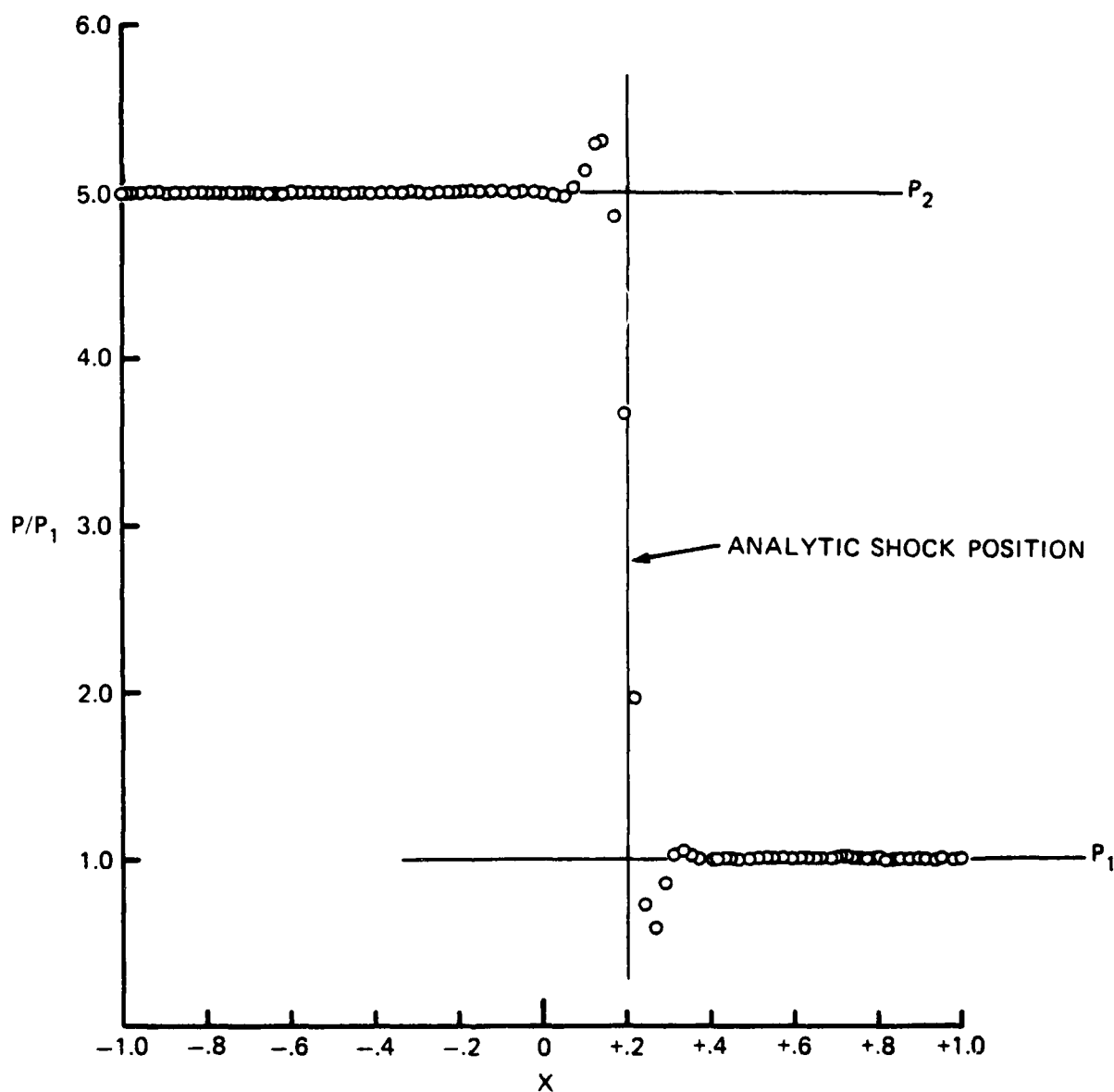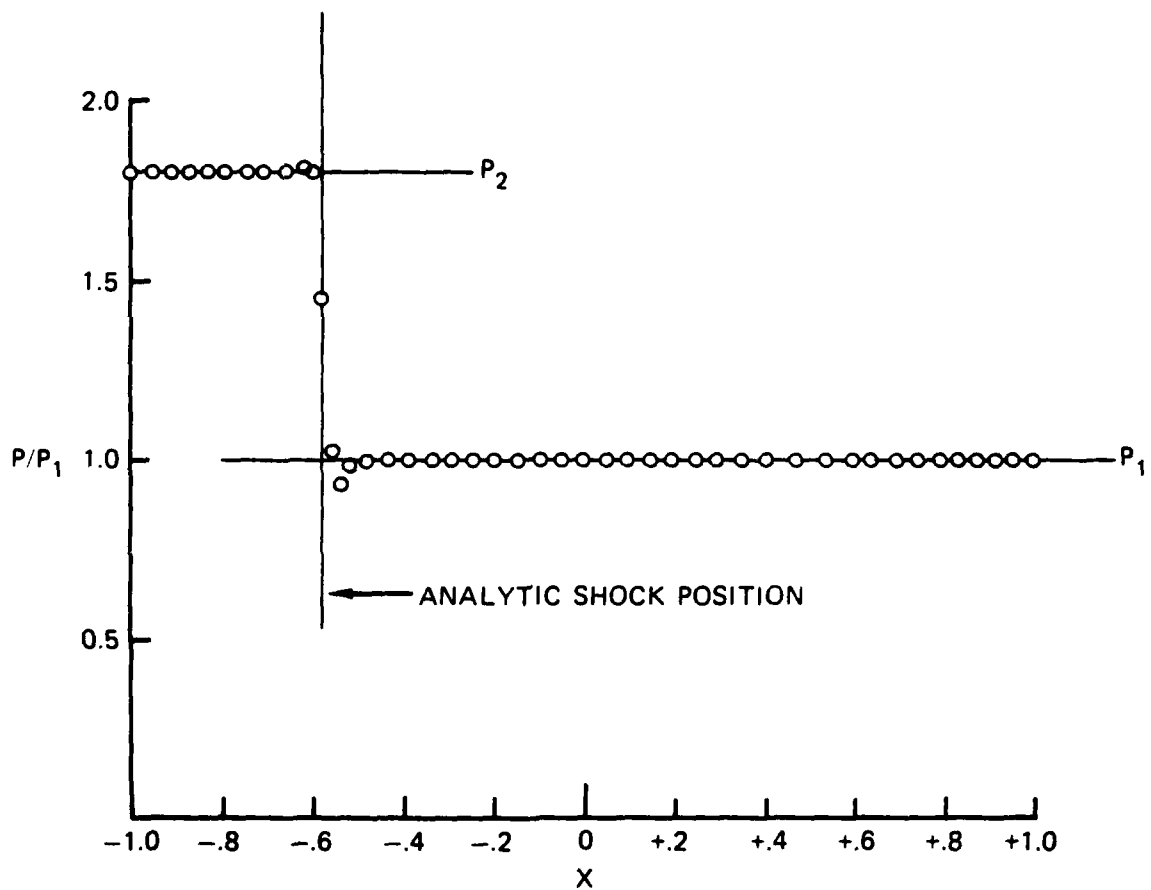
Fig. 5 — P/P_1 vs x at ITER = 1000, t = 0.0570 for supersonic inflow and subsonic outflow. MSHOCK = 2.94957, M1 = 0.84515, 4th order dissipation scheme.

17

Fig. 6 — P/P_1 vs x at ITER = 6000, t = 0.3448 for supersonic inflow and subsonic outflow. MSHOCK = 2.94957, M1 = 0.84515, 4th order dissipation scheme.

18

Fig. 7 — P/P_1 vs x at ITER = 2000, t = 0.1998 for subsonic inflow and outflow.
MSHOCK = 1.80, M1 = 0.50, 4th order dissipation scheme.
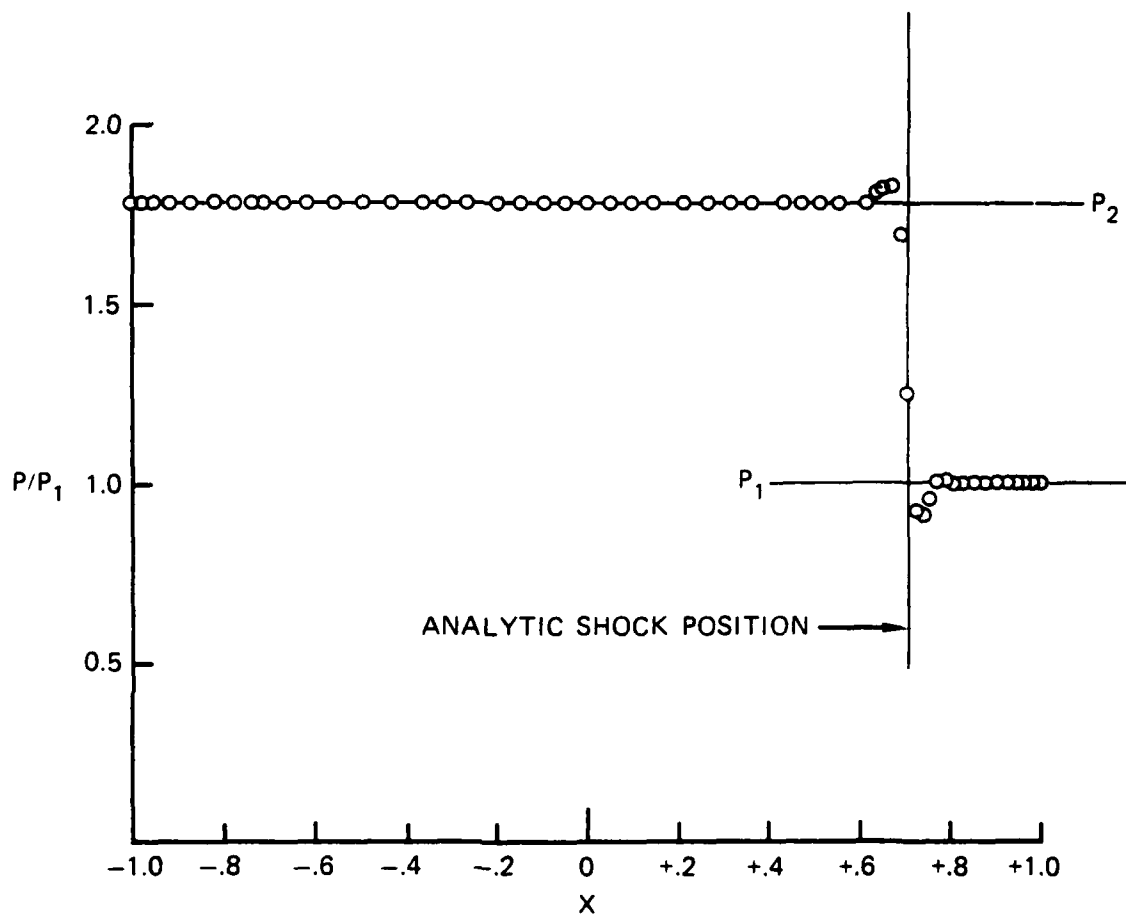
Fig. 8 — P/P_1 vs x at ITER = 8000, t = 0.7992 for subsonic inflow and outflow. MSHOCK = 1.80, M1 = 0.50, 4th order dissipation scheme.
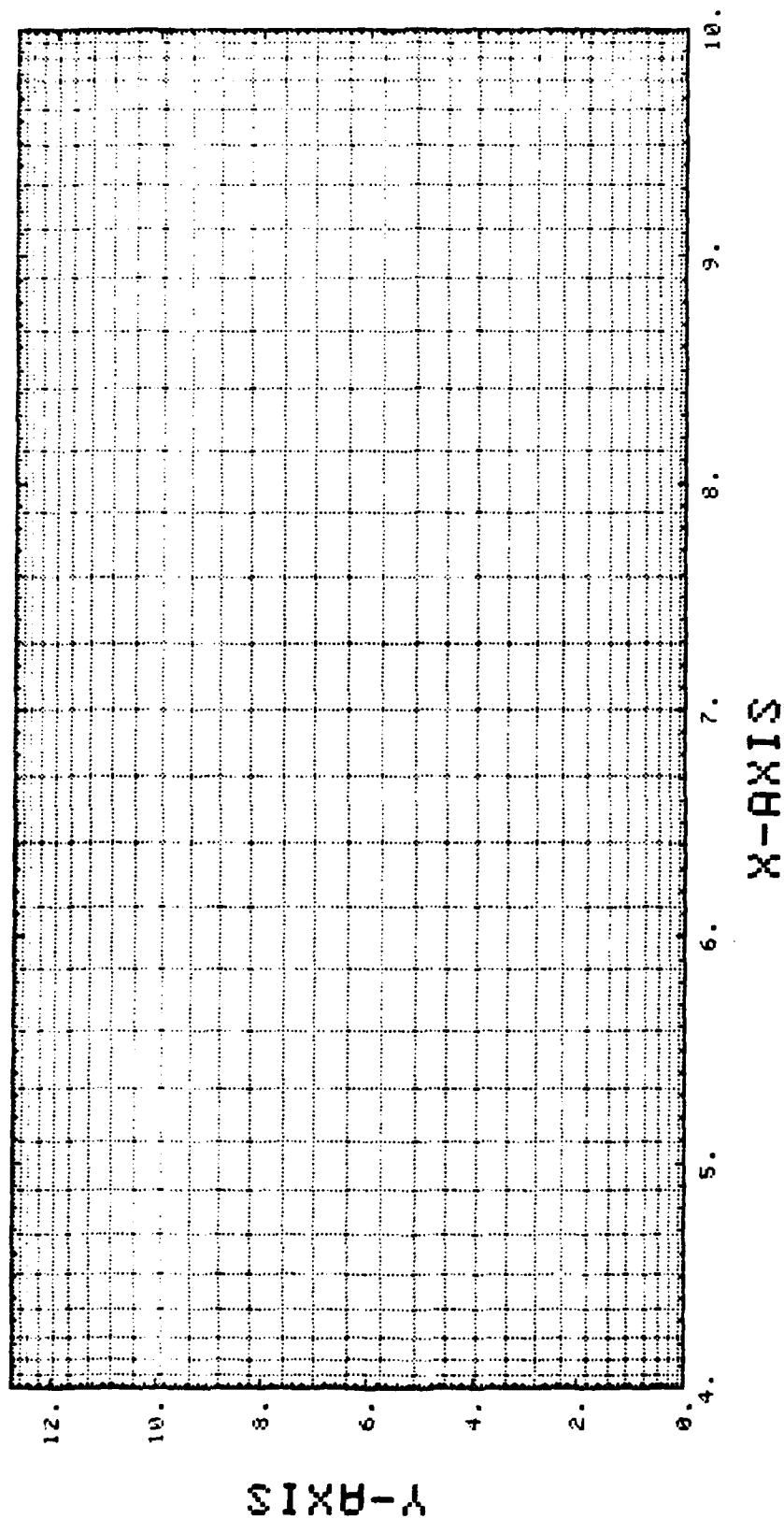
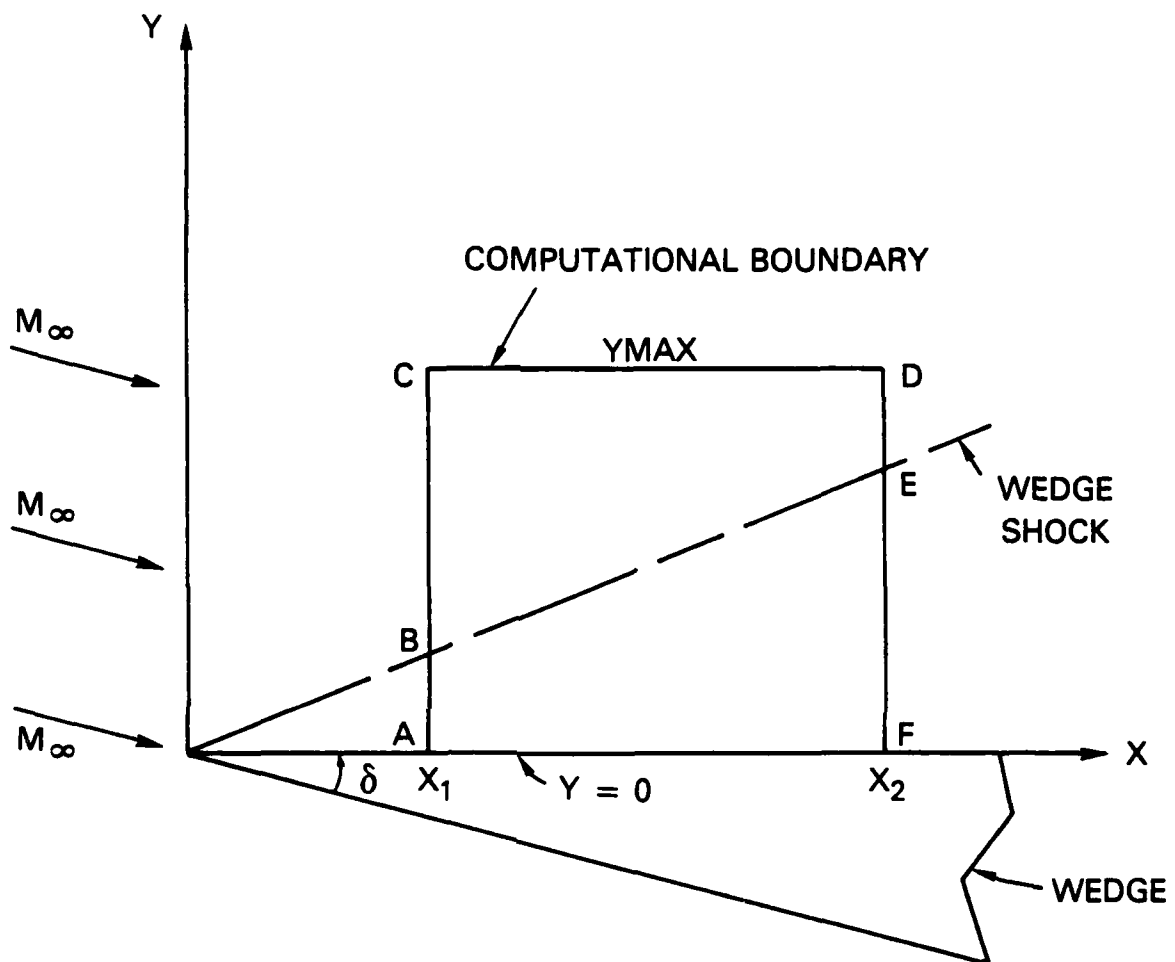**X-AXIS**

Y-AXIS

Fig. 9 — Computational grid for wedge flow calculations

21

Fig. 10 — Physical space computational boundary
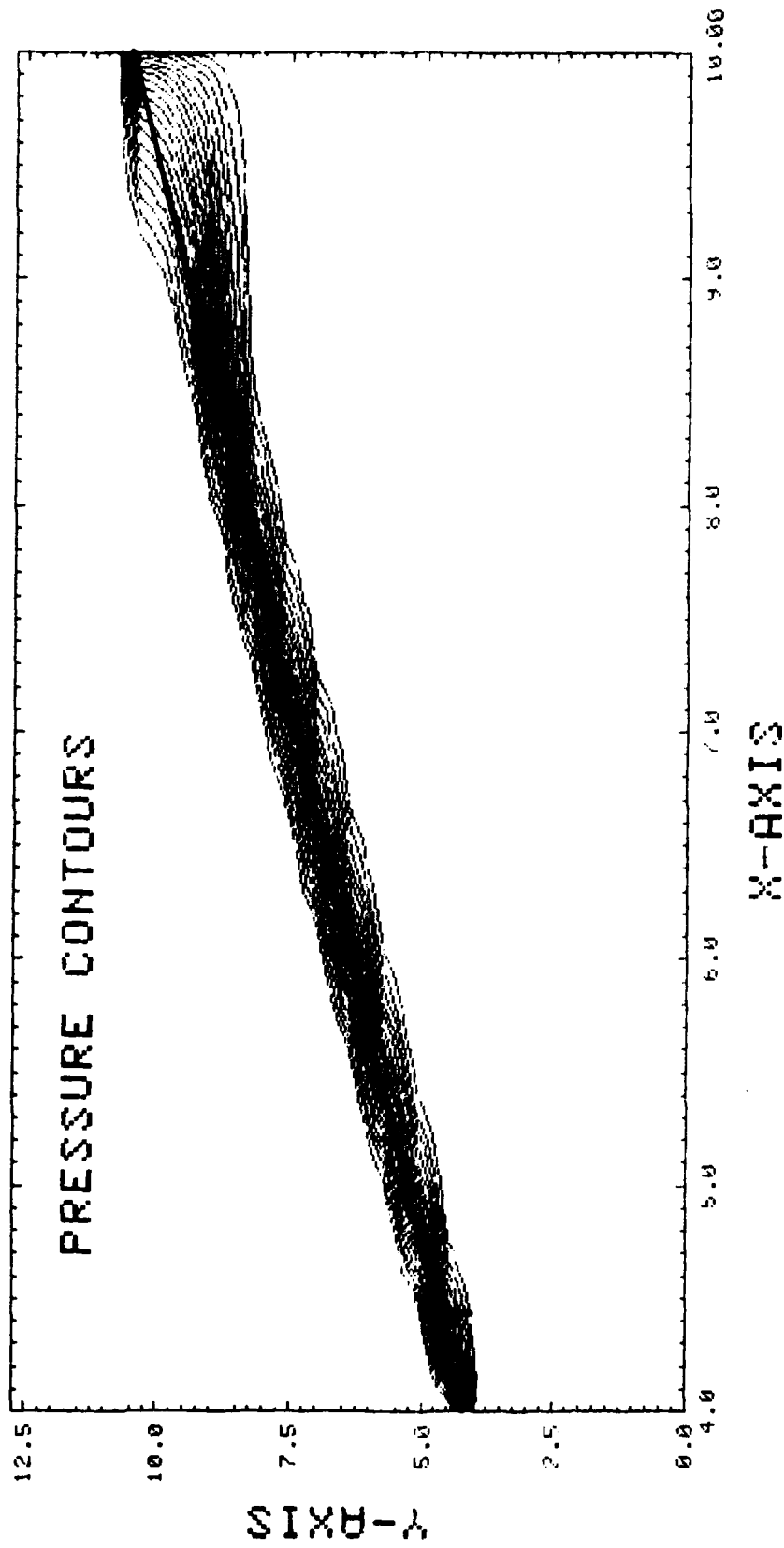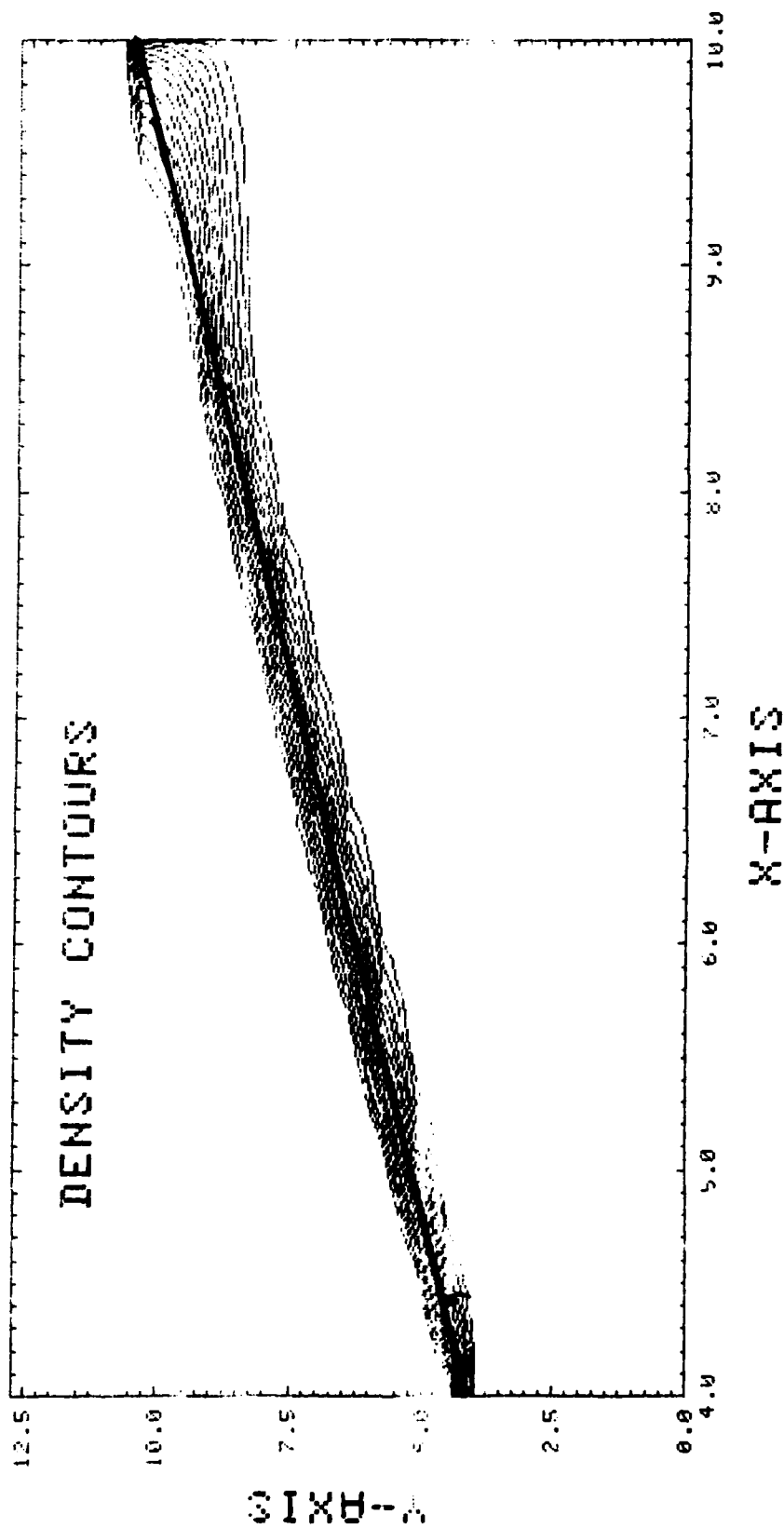
PRESSURE CONTOURS

X-AXIS

Fig. 11 — Supersonic wedge flow, M1 = 1.5, DELTA = 10°, 33 × 33 grid

DENSITY CONTOURS

X-AXIS

Y-AXIS

Fig. 12 — Supersonic wedge flow, M1 = 1.5, DELTA = 10°, 33 × 33 grid

24

MACH NO. = 1.50
DELTA = 10.00 DEGREES
GRID SIZE (NX, NY): 33 BY 33

X-AXIS

SURFACE PRESSURE

Fig. 13 — Comparison of analytic and calculated wedge surface pressure distributions

MACH NO. = 1.50
DELTA = 10.00 DEGREES
GRID SIZE (NX, NY): 33 BY 33
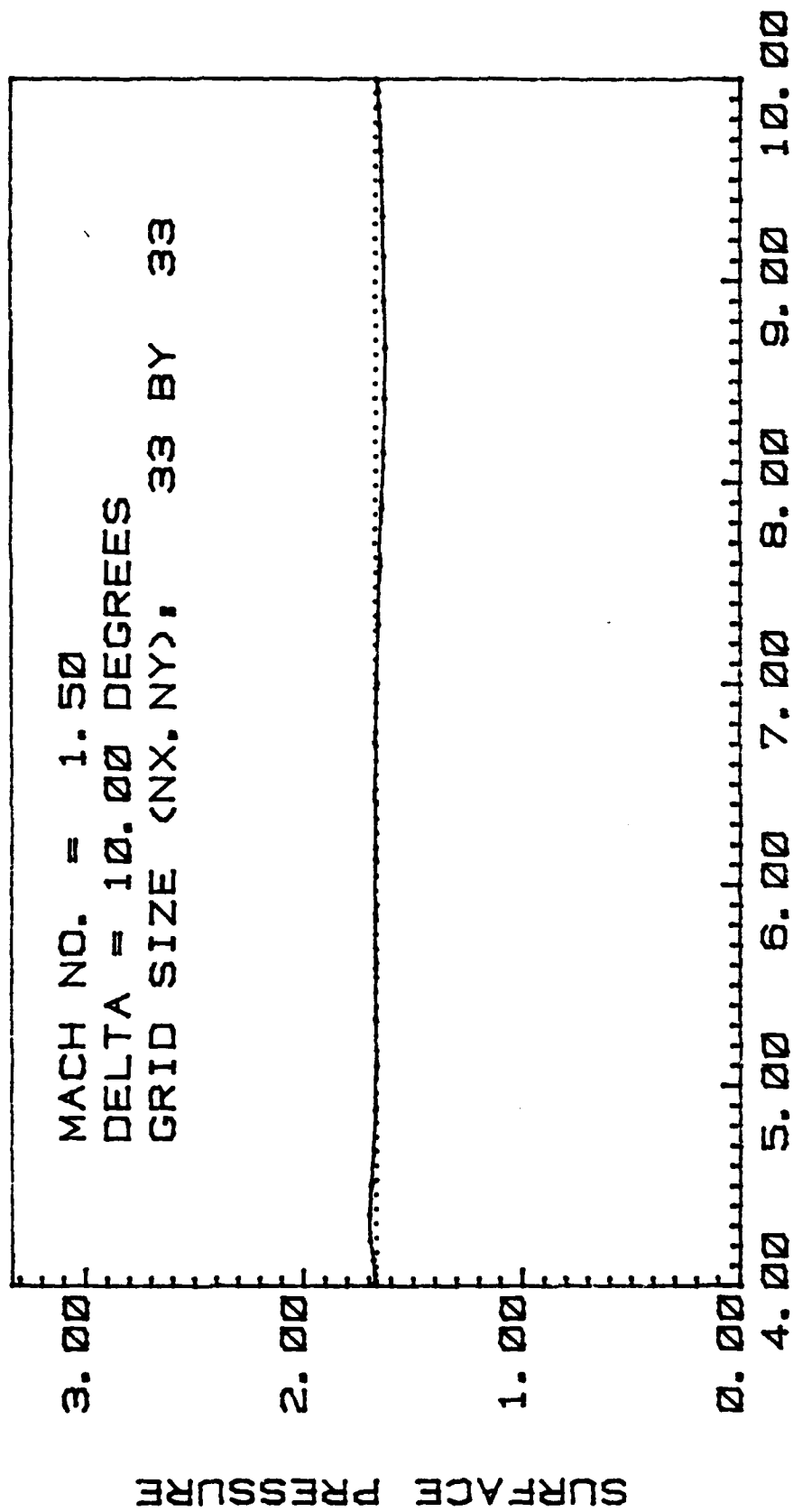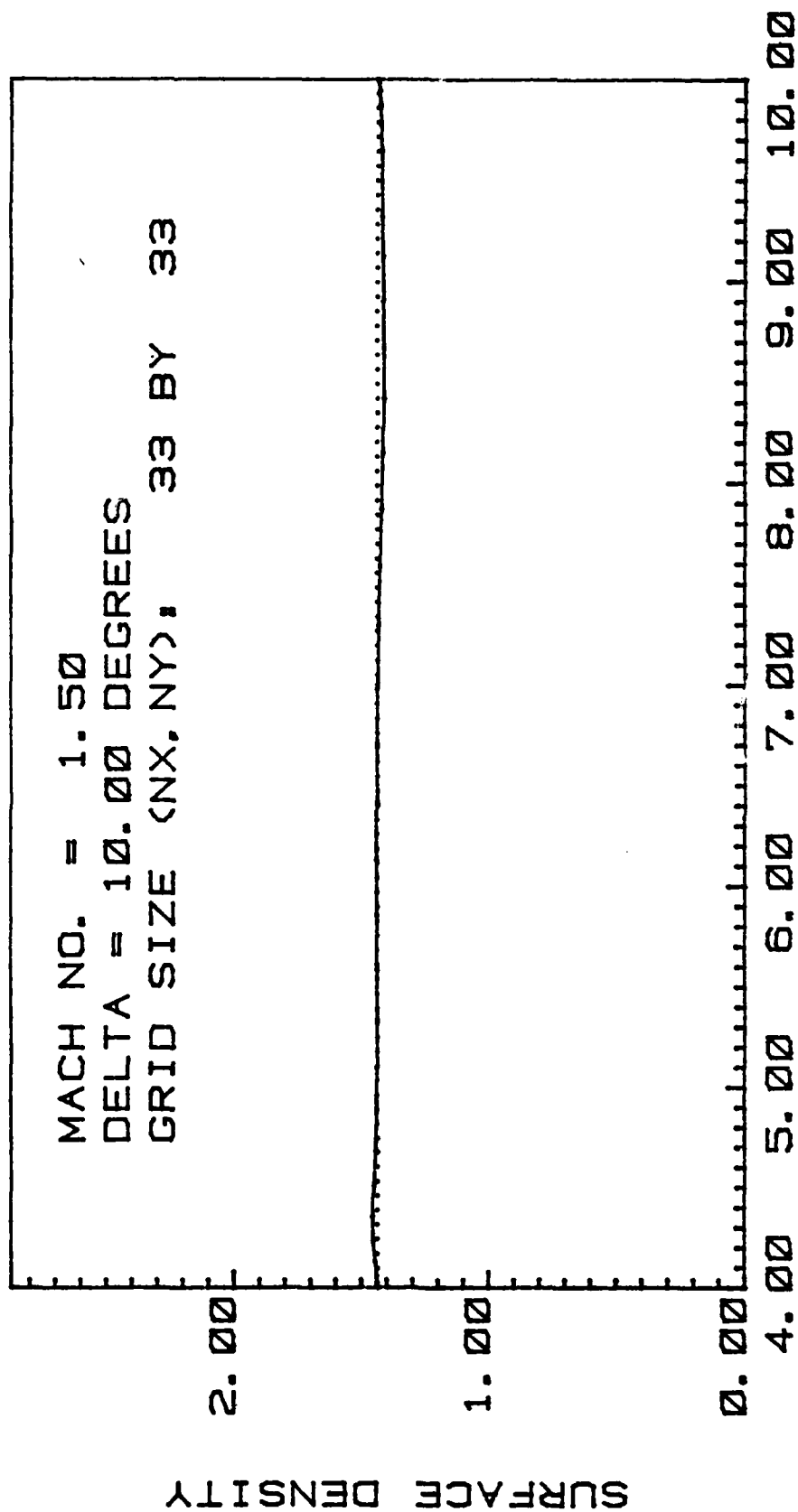
SURFACE DENSITY

X-AXIS

Fig. 14 — Comparison of analytic and calculated wedge surface density distributions

PRESSURE CONTOURS

MACH NO. =3.00

DELTA =10.00

Y-AXIS

X-AXIS

4.00   3.00   2.00   1.00   0.00
4.00   10.00

Fig. 15 — Supersonic wedge flow computed shock wave

27

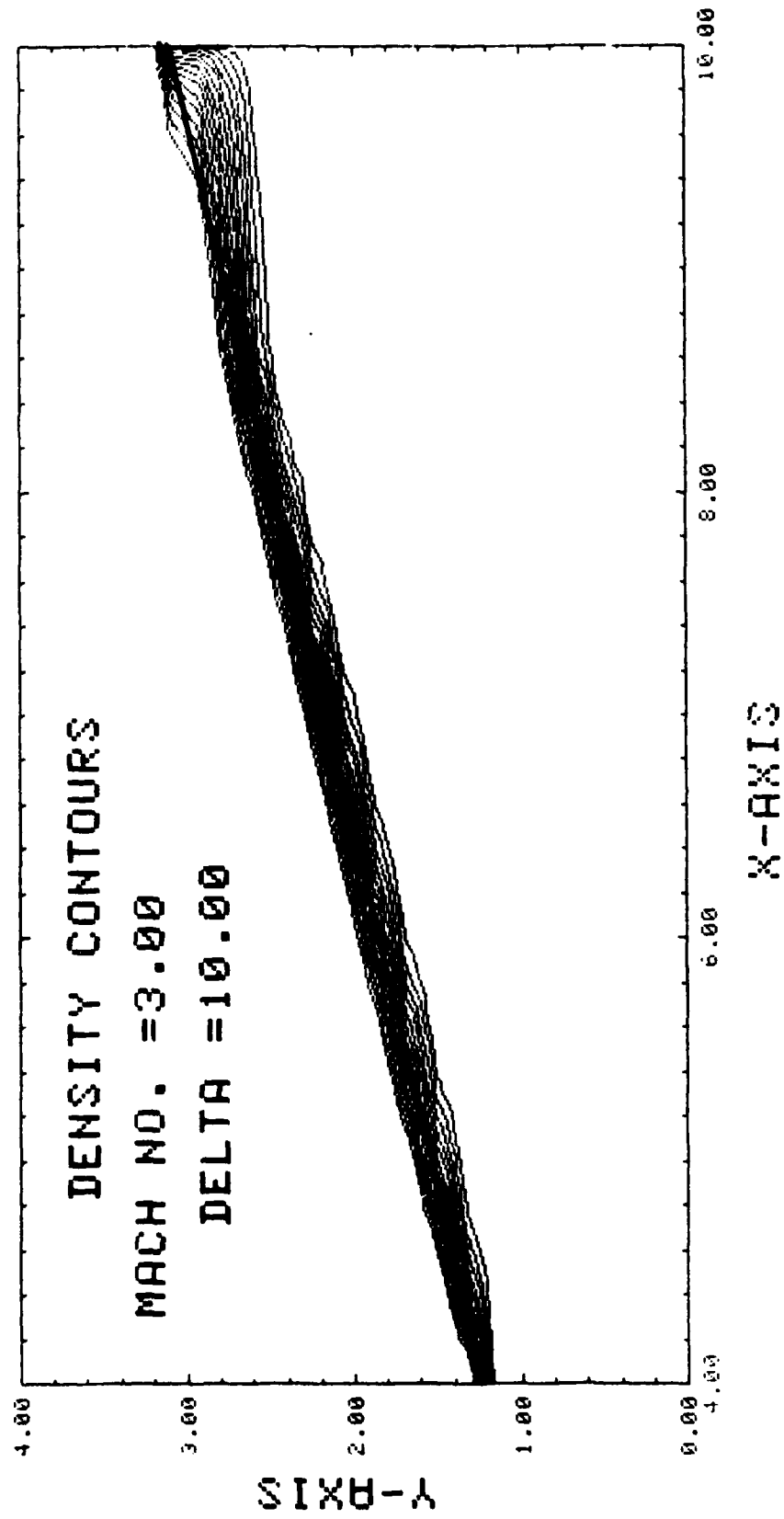DENSITY CONTOURS

MACH NO. =3.00

DELTA =10.00

X-AXIS

Y-AXIS
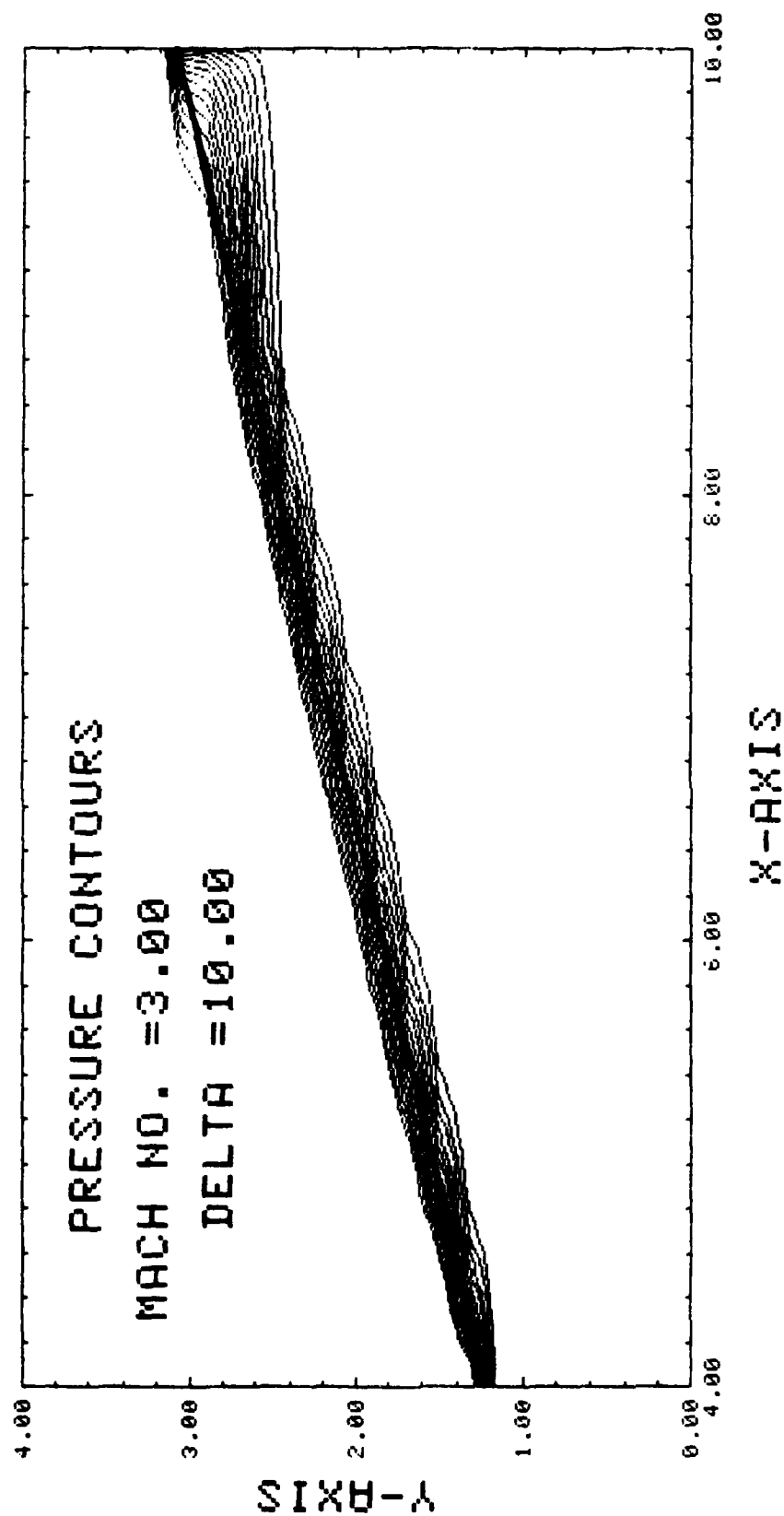
Fig. 16 — Supersonic wedge flow computed shock wave

28

Fig. 17 — Comparison of analytic and calculated wedge surface pressure distributions

MACH NO. = 3.00
DELTA = 10.00 DEGREES
GRID SIZE (NX,NY): 33 BY 33
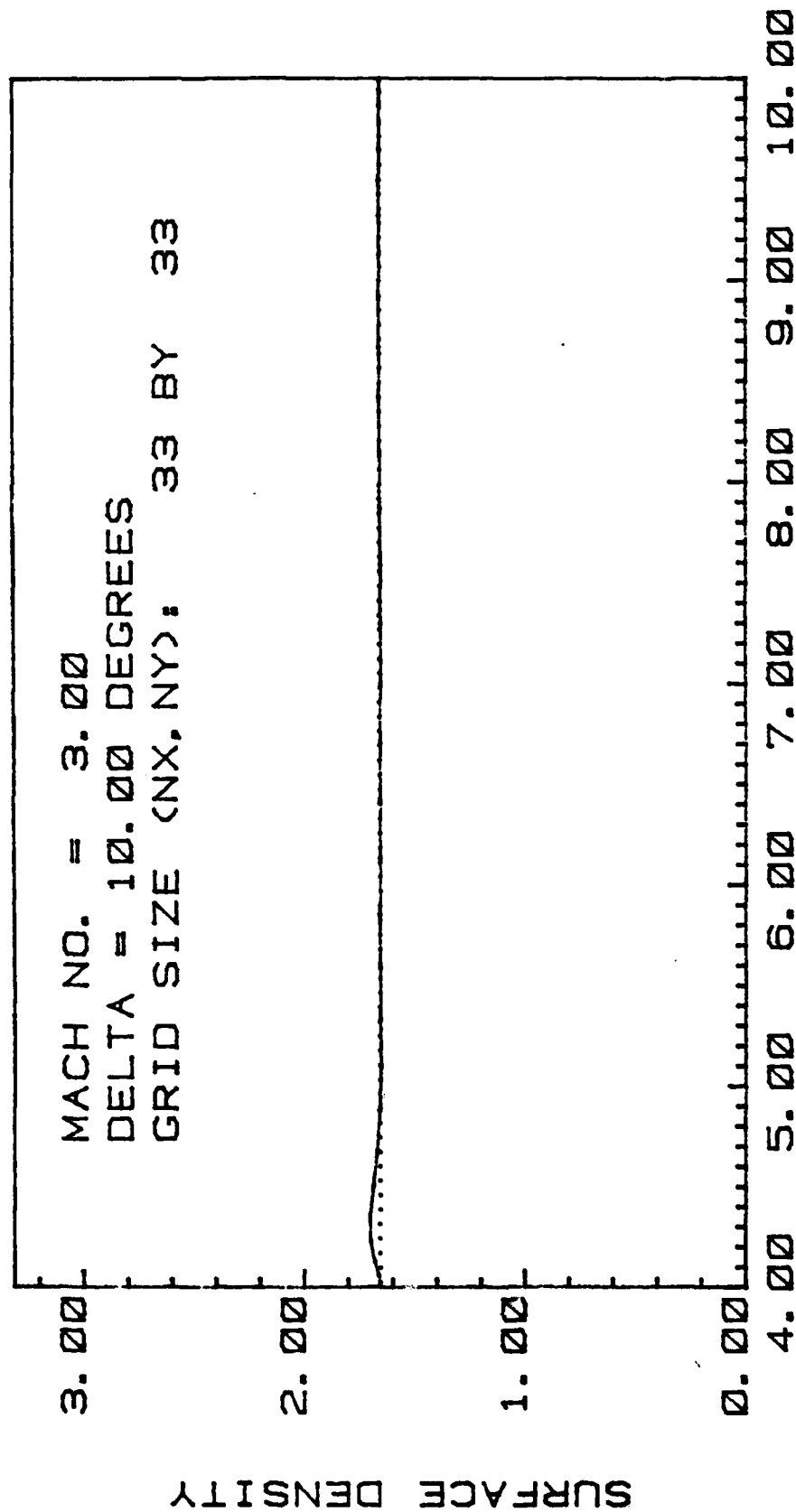
SURFACE PRESSURE

X-AXIS

Fig. 18 — Comparison of analytic and calculated wedge surface density distributions

MACH NO. = 3.00
DELTA = 10.00 DEGREES
GRID SIZE (NX,NY): 33 BY 33

X-AXIS

SURFACE DENSITY

6. REFERENCES

1. Taylor, T., Myers, R., and Albert, J. "Pseudospectral Calculations of Shock Waves, Rarefaction Waves and Contact Surfaces", technical note, Computers and Fluids, Vol. 9, No. 4, 1981.

2. Gottlieb, D., Lustman, L. and Orszag, S., "Spectral Calculations of One-Dimensional Inviscid Compressible Flows", SIAM J., Vol. 2, No. 3, September 1981.

3. Boris, J. and Book, D., "Solution of Continuity Equations by the Method of Flux-Corrected Transport", Methods in Computational Physics, Vol. 16, Academic Press, New York, 1976.

4. Gottlieb, D. and Orszag, S., Numerical Analysis of Spectral Methods: Theory and Applications, CBMS-NSF Regional Conference Series in Applied Mathematics, Monograph 26.

5. Gottlieb, D., private communication.